INTERNATIONAL ATOMIC ENERGY AGENCY
UNITED NATIONS EDUCATIONAL, SCIENTIFIC AND CULTURAL ORGANIZATION
INTERNATIONAL CENTRE FOR THEORETICAL PHYSICS
I.C.T.P., P.O. BOX 586, 34100 TRIESTE, ITALY, CABLE: CENTRATOM TRIESTE

H4.SMR/480-18

WORKSHOP ON EARTHQUAKE SOURCES
& REGIONAL LITHOSPHERIC
STRUCTURES FROM SEISMIC WAVE DATA

19 - 30 November 1990

A New Algorithm for Spline Approximation Tomography

D.E. Lokchtanov, A.L. Levshin, *G.F. Panza

International Institute of Earthquake Prediction
& Math. Geophysics of the USSR
Moscow, U.S.S.R.

*Università di Trieste
Istituto di Geodesia e Geofisica
Trieste, Italy

A new algorithm for spline approximation tomograpy

by

D.E.Lokchtanov, A.L.Levshin and G.F.Panza

ABSTRACT. A tomography algorithm, based on the ray perturbation method and 2D wave velocity distribution approximation with cubic B - splines is suggested. The splines are subjected to tension to remove undesireable oscillations of the approximating function in those parts of the investigated 2D region, that are poorly covered by seismic ray trajectories. The viability of the algorithm is investigated by numerical model examples and by processing of real observations of Rayleigh wave phase velocities in Western Europe. The reconstructed maps of phase velocity are in turn used for checking the tomography algorithm by comparing theoretical seismograms, calculated by ray perturbation and by Gaussian beams methods.

THE NEW ALGORITHM FOR SPLINE APPROXIMATION TOMOGRAPHY

D. Lokshtanov A. Levshin G. Panza

Here we extend the approach for 2-D function approximation, developed by Inoue (1986) for the tasks of tomography. We suppose, that 2-D distribution of wave velocity $c(x,y)$ weakly differs from the constant value, so the input data - travel times or phase shifts of wave signals are determined by integrals of slowness function $p(x,y)=1/c(x,y)$ along unperturbed straight rays. These travel times along rays, lying in 2-D plane, are used for reconstructing the function $p(x,y)$ on that part of the plane, which is covered by traces. The number of traces is not large and they are not regularly spaced, so it is impossible to use the methods, based on Radon transformation (Chapman,1987; Kak,1985). In such practical for seismology problems situations with a lack of traces the conventional approach consists in representation of unknown function $p(x,y)$ as a sum of basic functions. Then the task is reduced to estimation of basic functions coefficients by solution of system of linear algebraic equations (Nolet,1987; van der Sluis et al.,1987). Often the investigated part of the plane (or volume in 3-D case) is divided into rectangular cells and it is assumed, that velocity is constant inside each cell (Aki et al.,1977). To make solution more stable, the result is smoothed by introducing connections between velocities in cells, for example by means of priory covariance function (Tarantola et al.,1984). Sometimes, when it is known, that the reconstructing map is quite smooth function of coordinates, as in the case of long period surface waves group and phase velocities, instead of dealing with step basic functions, it is used Fourier or spherical harmonics expansion (Anderson,1984; Nakanishi et al.,1982). The lack of such approach is that inspite of different density of traces, in every point of investigated region the slowness is represented by the same number of basic functions, so the resulted slowness distribution has uniform detaility. This deficiency may be over come by using 2-D Backus - - Gilbert approach (Yanovskaya,1984). In such method the level of smoothness of solution depends in each point on local density of traces, but in the same time, the constructed basic functions have gaps of first and higher derivatives, and it must be possible to represent a reconstructed function $p(x,y)$ by a sum of two functions $p_1(x)$, $p_2(y)$,

depending on one coordinate.

Our approach for solving the tomography tasks is based on slowness function approximation by 2-D cubic B-splines. Such spline approximation is flexible to variety of 2-D smooth function shapes. By exploiting the locally basic functions, the solution may have different detaility in different points of investigated region. As in the work of Inoue, the splines are subjected to tension to remove undesireable oscillations in the parts, poorly covered by traces.

At first we describe the algorithm for spline approximation tomography. Then we show the numerical model results with the same set of traces, that are used later for determining Rayleigh wave phase velocity maps in western Europe. After this the resulted maps are used for checking the validity of the method by comparing theoretical phase shifts in spectra of seismograms, computed by ray perturbation and Gaussian beams method.

1. 2-D tomography with B-cubic splines.

Let us have the straight seismic traces l_i, that are lying in a rectangular plane domain Ω ($X_{min} \le x \le X_{max}$, $Y_{min} \le y \le Y_{max}$). For each trace we know the measurement result of the averaged value of the slowness p_i:

$$p_i = \frac{1}{L_i} \int_{l_i} p(l)\,dl + \xi_i , \qquad i=1,N , \qquad (1)$$

where L_i - the length of i-th trace, ξ_i - the error of measurement. The task is to reconstruct the function $p(x,y)$ in domain Ω from the results of measurements p_i. We suppose, that the function $p(x,y)$ is smooth with continueous first and second derivatives.

The function $p(x,y)$ will be approximated by the function $f(x,y)$, that is represented as a sum of M basic functions $\psi_k(x,y)$:

$$f(x,y) = \sum_{k=1}^{M} c_k \psi_k(x,y) . \qquad (2)$$

When the basic functions are 2-D cubic B - splines, the functions $\psi_k(x,y)$ are determined by the following manner (Inoue,1986; de Boor,1978) .

Let $\Delta_x = (X_{max} - X_{min})/M_x$, $\Delta_y = (Y_{max} - Y_{min})/M_y$, where M_x and M_y are integer values, such as $M_x \ge 1$, $M_y \ge 1$. Consider a rectangular grid , that is created by lines $x = const = X_{min} + i\Delta_x$, and $y = const = Y_{min} + j\Delta_y$, $i=-1,M_x+2$, $j=-1,M_y+2$. Every grid knot is associated with a basic function $F_{ij}(x,y) = F_i(x)F_j(y)$, where

$$F_i(x) = \begin{cases} 0, & x<Q_0 \\ B_1[(x-Q_0)/\Delta_x], & Q_0 \le x<Q_1 \\ B_2[(x-Q_1)/\Delta_x], & Q_1 \le x<Q_2 \\ B_3[(x-Q_2)/\Delta_x], & Q_2 \le x<Q_3 \\ B_4[(x-Q_3)/\Delta_x], & Q_3 \le x<Q_4 \\ 0, & Q_4 \le x \end{cases} \qquad (3)$$

and

$$Q_l = X_{min} + (i+l-2), \qquad l=0,4 \quad , \qquad (4)$$

and

$$\begin{aligned} B_1(r) &= r^3/6 \ , \\ B_2(r) &= (-3r^3 + 3r^2 + 3r + 1)/6, \\ B_3(r) &= (3r^3 - 6r^2 + 4)/6, \\ B_4(r) &= (-r^3 + 3r^2 - 3r + 1)/6, \end{aligned} \qquad (5)$$

The function $F_j(y)$ is determined in a similar manner.

In accordance with introduced definitions, the formula (2) may be rewritten in the next form :

$$f(x,y) = \sum_{i=-1}^{M_x+2} \sum_{j=-1}^{M_y+2} c_{ij} F_{ij}(x,y). \qquad (6)$$

The coefficients c_{ij} are determined from the condition of minimum the functional

$$P = \sum_{i=1}^{N} w_i (p_i - p_i^{obs})^2 + R_1 + R_2 \ , \qquad (7)$$

where

$$R_1 = W_1 \int\int_{\Omega} [(\frac{\partial f}{\partial x})^2 + (\frac{\partial f}{\partial y})^2] dxdy \ , \qquad (8)$$

$$R_2 = W_2 \int\int_{\Omega} [(\frac{\partial^2 f}{\partial x^2})^2 + 2(\frac{\partial^2 f}{\partial x \partial y})^2 + (\frac{\partial^2 f}{\partial y^2})^2] dxdy \ , \qquad (9)$$

w_i, W_1, W_2 - weights,

$$p_i = \frac{1}{L_i} \int_{l_i} f(x,y) dl. \qquad (10)$$

The introduction in the functional (7) the regularizing addendums R_1 and R_2 dampers unwanted oscillations of $f(x,y)$ in these parts of Ω, that are poorly covered by traces. The functional (7) has the same form as that one, used for finding configuration of 2-D elastic bar with flexural rigity D under tension T. This bar is pulled laterally to points $(x_i \ , \ y_i, \ d_i)$ by zero free length springs of stiffness k_i . The configuration of the bar $f(x,y)$ is determined from the condition of minimum strain energy of the system :

$$U = \sum_{i=1}^{N} \frac{k_i}{2} (f_i - d_i)^2 + \int\int_{\Omega} [T/2[(\frac{\partial f}{\partial x})^2 + (\frac{\partial f}{\partial y})^2] +$$

$$+ D/2[(\frac{\partial^2 f}{\partial x^2})^2 + 2(\frac{\partial^2 f}{\partial x \partial y})^2 + (\frac{\partial^2 f}{\partial y^2})^2]] \ dx \ dy \ .$$

The parameters M_x , M_y and weights W_1, W_2 in (6) and (8),(9) may be chosen from the next considerations. When W_1, W_2 increase and M_x , M_y decrease, the dispersion of the estimates of slowness values also decreases But in the same time increases biasedness of the estimates of slowness values with respect to some reference model, for example homogeneous one. The optimal values of these parameters may be found from the condition of minimum the total expected estimation error.

The minimization of (7) over c_{ij} is equivalent to solving the system of linear algebraic equations with matrix $N_m \times N_m$, where $N_m = (M_x+3) \times (M_y+3)$.

2. Numerical examples.

The algorithm was used for analysis of Raileigh wave phase velocities in Western Europe (Panza et al.,1980). Before to present the processing results we show the results of model experiments with the same set of traces.

Our algorithm is based on approximation of 2-D function by cubic splines in Cartesian coordinate system. So, first of all, it is necessary to transform initial data for spherical Earth to the data for flat model. We use the following transformation

$$\begin{aligned} x &= R_0 \ ln \ tg(\theta/2) \ , \\ y &= R_0 \ \varphi \ , \\ V(x,y) &= v(\theta,\varphi)/\sin\theta, \end{aligned} \qquad (11)$$

that preserves the wave travel time between corresponding points (Yanovskaja, 1982). In these formulas R_0 - the Earth radius, $\theta = \pi/2 - \psi$,

ψ is latitude and φ is longitude.

The initial data for the tomography algorithm are the values of slownesses, averaged along the unperturbed straight rays.For such approach validity it is necessary, that velocity would change in the region of interest as slow as possible. For this, when the transformation (11) is used, the area under consideration is moved to equator, where $\frac{\partial}{\partial\theta}(\sin\theta)=0$. After we get the result in Cartesian coord i nate system, by transformations reverse to (11) we have an answer in spherical coordinates

The first model example was processed for the media with constant velocity, $c^{mod}=3.75$. The traces geometry (after transformation (11)) is shown on fig. 1. As was mentioned above, these traces correspond to real traces, that were used for analysis of Rayleigh wave dispersion in Western Europe. The results of tomography are shown on fig.2 . Inside the region the estimates are practically the same as true velocities. Near the boder, where the area is poorly covered by traces, and the surface $p(x,y)$ aspires to occupy position with " minimum strain energy " the result differs significantly from the true model.

In the second model example the model velocity was computed by formula $c^{mod}= 1./(0.25 + 0.5\sin(2\pi x/T_x)\sin(2\pi y/T_y))$, where $T_x= X_{max}- X_{min}$, $T_y= Y_{max}- Y_{min}$. The lines of equal levels for the true model and the result of tomography are shown on fig.3 . Despite of small density of traces, inside of the area, we get quite good agreement between the true and resulted models. In both examples and following computations for real data the slowness function approximated by 16 (4x4) 2-D cubic B-splines.

3. The results of real data analysis

Now we discuss the results of real data analysis. These data are averaged values of Rayleigh wave phase velocities for traces, shown on fig.1. The available periods are 25, 50 and 80 seconds .The results of tomography are presented on fig.4. These results are very similar to those, obtained in previous investigations (Yanovskaja et al., 1990; Panza et al.,1980; Calcagnile et al.,1981).

In accordance with (1), the used algorithm is based on computation of phase delay along unperturbed ray. Therefore, for the resulted velocity maps it's very important to check the validity of such computations. For this we compaired the synthetic phase slownesses , calculated by Gaussian beams technique (Yomogida, 1985) and by formula (10). During

computations with Gaussian beams method, for each pair of stations, lying approximately on the same greate circle with the source, we determined phase spectrum and then calculated the average slownesses by formula

$$p^{aver} = \Delta\varphi \,/\, (2\pi f \Delta R) , \qquad (12)$$

where $\Delta\varphi$ - the phase difference, ΔR - the distance between stations, f - frequency.

So far as we know the maps of phase velocity only for the investigated region, for the Gaussian beams computations it's necessary, that the source is located in the same region. Therefore from the all events, used in this work, we selected two, that satisfy this condition (Tabl. 1). Besides the information about phase velocity distribution, we also must know the structure in the vicinity of recievers and sources for eigenfunctions computation. For this we used the simplest models - the layer over halfspace, with theoretical phase velocities, compatible with the results of tomography (Tabl.2).

The results of computations by described two methods are given in the tabl.3 . The averaged phase slownesses, received by pertutbed ray method and by Gaussian beams method are in a good agreement with each other. Notice, that in spite of bigger variations of velocity function for 25 sec than for 50 sec, the difference between average slowness, computed by two methods, are of the same order for both periods. Obviously,it is connected with larger Fresnel zone fore larger periods. We have not made such comparison for T=80 sec., because for this period variations of slowness function are comparable with the errors of initial data.

Conclusions.

In the paper we extended the approach for 2-D function approximation with cubic B-splines to the tasks of tomography. The tomography algorithm was checked by numerical model examples and real data processing. The reconstructed maps of Rayleigh wave phase velocity in Western Europe were used for controlling the validity of using tomography algorithms, based on computation phase delays of propagated wave signals along unperturbed straight rays.

References

Aki,K.,Christoffersson,A.,Husebye,E.S.,1977, Determination of the three-dimensional seismic structure of the litospere: J.Geopys. Res.,82, 277-296.

Anderson,D.L.,Surface wave tomography: Trans.Amer.Geophys. Union, 1984, 65, 147-148.

Calcagnile,G.,Panza,G.F.,1981, The main characteristics of the lithosphere - asthenosphere system in Italy and surrounding regions: Pure Appl. Geophys.,119, 865-879.

Chapman,C.H.,1987.The Radon transform and seismic tomography: Seismic tomography,G.Nolet (ed.),D. Reidel Publishing Company.

de Boor,C.,1978. A practical guide to splines: Springer-Verlag.

Inoue,H.,1986, A least-squares smooth fitting for irregularly spaced data: Finite-element approach using the cubic B-spline basis: Geophysics, 51, 2051-2066.

Kak,A.C.,1985. Tomographic imaging with diffracting and nondiffractind sources:Array signal processing,S.Haykin (ed.),Prentice--Hall,Inc.

Nakanishi,I., Anderson,D.L., 1982,World-wide distribution of group velocity of mantle Rayleigh waves as determined by spherical inversion: Bull. Seismol. Soc. Amer., 72, 1185-1194.

Nolet,G.,1987.Seismic wave propagation and seismic tomography:Seismic tomography,G.Nolet (ed.),D. Reidel Publishing Company.

Panza,G.F.,Mueller,St. and Calcagnile,G.,1980, The gross features of the lithosphere-asthenosphere system in Europe from seismic surface waves and body waves: Pure Appl. Geophysics,118, 1209--1213.

Tarantola,A. and Nercessian,A.,1984, Three-dimensional inversion without blocks: Geophys.J.R.astr.Soc.,76,299-306.

van der Sluis,A. and van der Vorst H.A.,1987. Numerical solution of large, sparse linear algebraic systems arizing from tomography problems: Seismic tomography, G.Nolet (ed.), D. Reidel Publishing Company.

Yanovskaya,T.B.,Panza,G.F., Ditmar,P.G., Suhadolc,P., Mueller,St., 1990, Structural heterogeneity and anizotropy based on 2-D phase velocity patterns of Rayleigh waves in Western Europe, (in press).

Yanovskaya,T.B.,1984,Solution of the inverse problem of seismology for laterally inhomogeneous media: Geophys.J.Roy.astr.Soc., 79, 293-304.

Yanovskaya,T.B.,1982,Distribution of surface wave group velocities in North Atlantic: Izv. AN SSSR, Fizika Zemli, 2, 3-11

Yomogida,K.and Aki,K.,1985. Waveform synthesis of surface waves in a laterally heterogeneous Earth by the Gaussian beam method: J.Geophys.Res.,90,7665-7688.

Table 1. The events parameters.

Date	Origin time	Coordinates	Magn.	Depth	Station pair
6/5-61	16 04 33.1	37.4N 11.2E	5.4	79	BES-MON
24/2-73	15 22 09.8	36.1N 4.4E	6.3	33	MLS-SGR

Table 2. The stations structure models.
For all stations $\alpha_i = 1.73\ \beta_i$, $\rho_1 = 2.9$, $\rho_2 = 3.3$

Station	Coordinates	The model parameters		
		β_1 (km/sec)	h_1 (km)	β_2 (km/sec)
BES	47 14 59N 05 59 15E	3.55	31.	4.45
MON	43 43 50N 07 25 33E	3.56	38.	4.45
SGR	47 42 32N 00 55 01E	3.83	35.5	4.52
MLS	42 57 29N 01 04 59E	3.76	34.5	4.46

Table 3. The results of average slowness computation (sec/km)

Station pair	Gaussian beams		Straight ray	
	T=25sec	T=50sec	T=25sec	T=50sec
BES-MON	0.2740	0.2548	0.2750	0.2564
MLS-SGR	0.2624	0.2465	0.2621	0.2472

Figures explanations

1. The geometry of traces, used for model experiments and real data processing. Each trace corresponds to the pair of seismic stations, lying approximately on the same great circle with the source.

2. The resulted velocity distribution for the model example with constant true velocity.

3. The resulted and true velocity maps for the second model experiment.

4. The reconstructed maps of phase velocities in Western Europe.

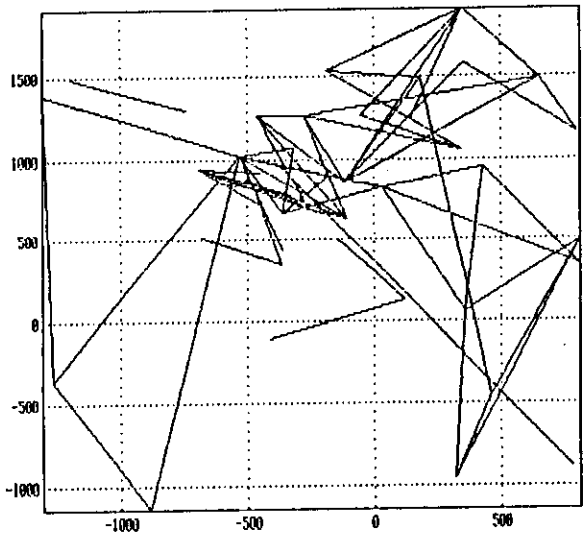
1500
1000
500
0
-500
-1000
-1000
-500
0
500

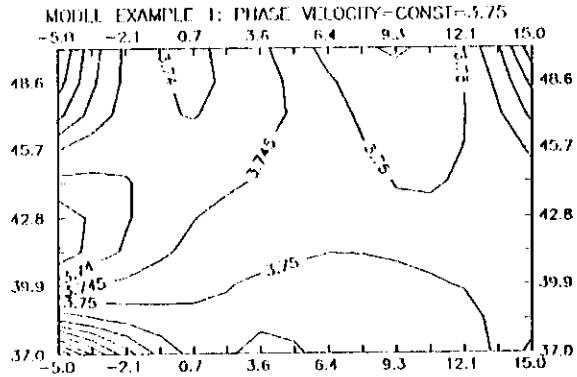
MODEL EXAMPLE 1: PHASE VELOCITY=CONST=3.75
-5.0
-2.1
0.7
3.6
6.4
9.3
12.1
15.0
48.6
45.7
42.8
39.9
37.0
3.745
3.75

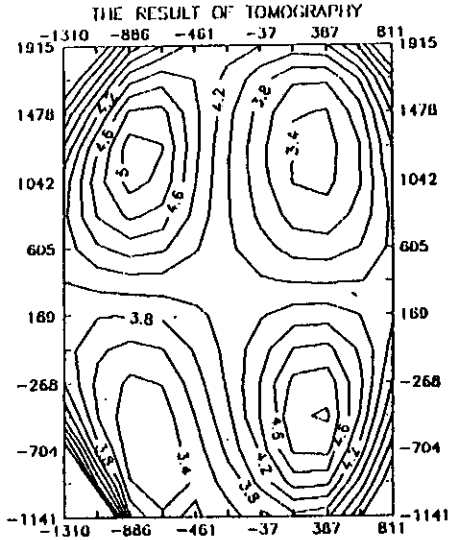
THE RESULT OF TOMOGRAPHY
-1310 -886 -461 -37 387 811
1915 1478 1042 605 169 -268 -704 -1141
4.4 4.2 3.8 4.6 5 3.4 4.6 3.8 4.6 4.2 4.4 3.4 3.9

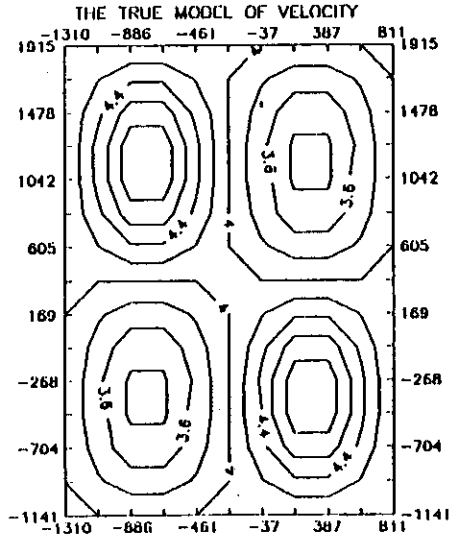
THE TRUE MODEL OF VELOCITY
-1310 -886 -461 -37 387 811
1915 1478 1042 605 169 -268 -704 -1141
4.4 4.4 3.6 4 3.6 4.4 4.4 4

Fig 3

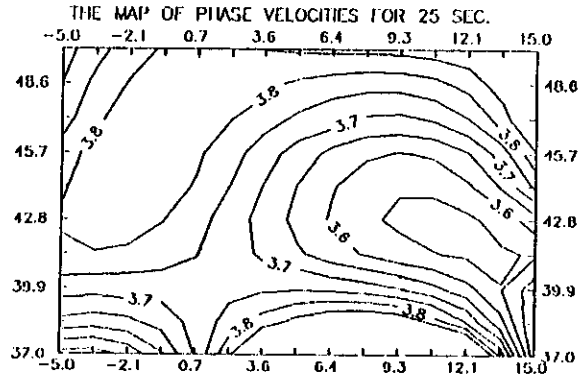
THE MAP OF PHASE VELOCITIES FOR 25 SEC.
-5.0 -2.1 0.7 3.6 6.4 9.3 12.1 15.0
48.6 45.7 42.8 39.9 37.0
3.8 3.7 3.6

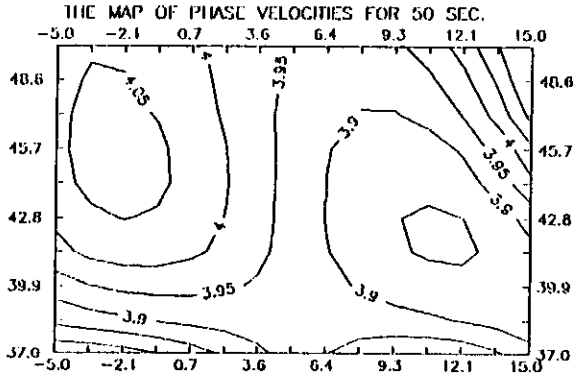
THE MAP OF PHASE VELOCITIES FOR 50 SEC.
-5.0 -2.1 0.7 3.6 6.4 9.3 12.1 15.0
48.6 45.7 42.8 39.9 37.0
4.05 4 3.95 3.9

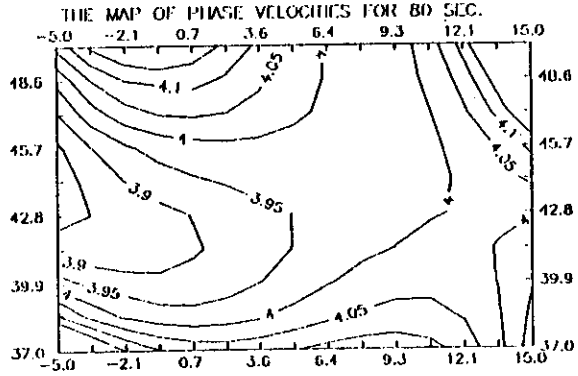
THE MAP OF PHASE VELOCITIES FOR 80 SEC.
-5.0 -2.1 0.7 3.6 6.4 9.3 12.1 15.0
48.6 45.7 42.8 39.9 37.0
4.1 4.05 4 3.95 3.9

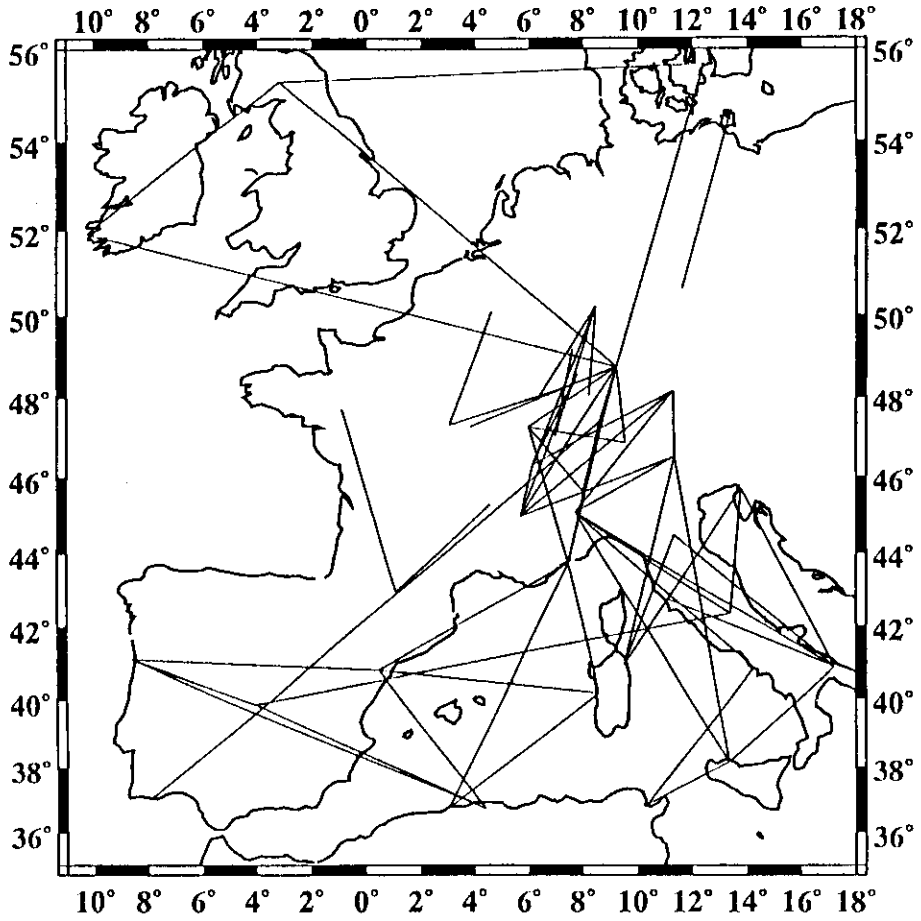

Fig. 1